Experimental Thermal and Fluid Science 46 (2013) 103–110

Contents lists available at SciVerse ScienceDirect

Experimental Thermal and Fluid Science

journal homepage: www.elsevier.com/locate/etfs

Effects of pulsing frequency on characteristics of electrohydrodynamic inkjet using micro-Al and nano-Ag particles

Min Wook Lee [a], Seongpil An [a], Na Young Kim [a], Ju Hyeoung Seo [a], Joo-Youl Huh [b], Ho Young Kim [a], Sam S. Yoon [a,*]

[a] School of Mechanical Engineering, Korea University, Seoul 136-713, Republic of Korea
[b] Department of Materials Science and Engineering, Korea University, Seoul 136-713, Republic of Korea

ARTICLE INFO

Article history:
Received 20 July 2012
Received in revised form 19 October 2012
Accepted 27 November 2012
Available online 20 December 2012

Keywords:
Electrohydrodynamic inkjet
Micro-nano-particle
Microdripping
Dot print

ABSTRACT

Characteristics of electrohydrodynamic inkjet were examined upon varying the applied voltage and frequency as well as the base-fluid. Low-cost inks are sought and micro-aluminum particle suspensions are candidates. Inclusion of large particles engendered satellite droplets and hence degraded print quality. However, the formation of satellite droplets can be prevented by increasing fluid's viscosity. Droplet sizes were measured as functions of the frequency; the higher the frequency, the smaller the droplet size. The low-cost inks with aluminum particles yielded reasonable performance on comparison with the expensive commercial ink comprised of silver nano-particles in case of printing dots that are a few hundred microns in size.

1. Introduction

Inkjet technologies have broad industrial applications in printed electronics, drug discovery, and micromechanical devices because of their fast and efficient operation, relative low cost, and capability to print highly complex pattern in mass production scale [1–4]. Inkjet droplet size can be tuned (known as "droplet-on-demand") by varying nozzle design and operating conditions [5–8] such that a range of micro-sized droplets can be deposited onto various substrates (i.e., paper, glass, silicon wafers, aluminum, and stainless steel). When the ink is replaced with fluids containing highly conducting particles, electrodes can be printed [9–11]. Printed electronics can benefit from the inkjet technology because of the: (1) ability to pattern various materials (either dissolved chemicals or colloidal metals), (2) compatibility with large-area substrates, (3) accurate targeting (high resolution), (4) relatively simple application (compared to photolithography), (5) potential for flexible, stretchable, roll-to-roll processes, and (6) potential non-vacuum and non-contact printing. Inkjet technology is already used in various industrial applications [12–14].

For printed electronics applications, inks comprised of silver nanoparticles are often used, which is expensive. Alternative inks at lower material cost and yet provide comparable performance should be sought. To avoid highly expensive manufacturing cost, the expense could be reduced through use of micro-sized aluminum (or copper) particles rather than nano-sized silver particles. Larger particles require a larger nozzle; however, the use of larger nozzles increases droplet size, which is unacceptable for micro-scale applications. Fortunately, an electrohydrodynamics (EHD) inkjet can produce droplets that are much smaller than the nozzle diameter. While there is a large body of literature covering EHD printing techniques [15–20], specific hydrodynamic aspects, such as droplet-size control and jetting behavior, have not been well understood. Also, studies on the effects of particle concentration on jetting behavior are rare. Furthermore, few have examined the characteristics of the printed dots (or relics) as a function of particle concentration.

In this effort, we investigated how dc-pulsed EHD jetting characteristics vary with pulsing frequency, particle concentration, and the solvents thermo-physical properties. While varying particle concentrations (Al weight %), relics (deposited droplets) were further examined with a scanning electronic microscope to help determine if printed dots and lines have potential for printed electrodes.

2. Materials and methods

Fig. 1 illustrates EHD jetting behavior. A Taylor cone forms at the nozzle tip under the actions of surface tension and electrostatic stresses on the surface of an equipotential cone [21]. A conical surface is formed when charge accumulates charges at the cone apex. This phenomenon leads to the surface destabilization and

* Corresponding author. Tel.: +82 (2) 3290 3376; fax: +82 (2) 926 9290.
E-mail address: skyoon@korea.ac.kr (S.S. Yoon).

0894-1777/$ - see front matter © 2012 Elsevier Inc. All rights reserved.
http://dx.doi.org/10.1016/j.expthermflusci.2012.11.025

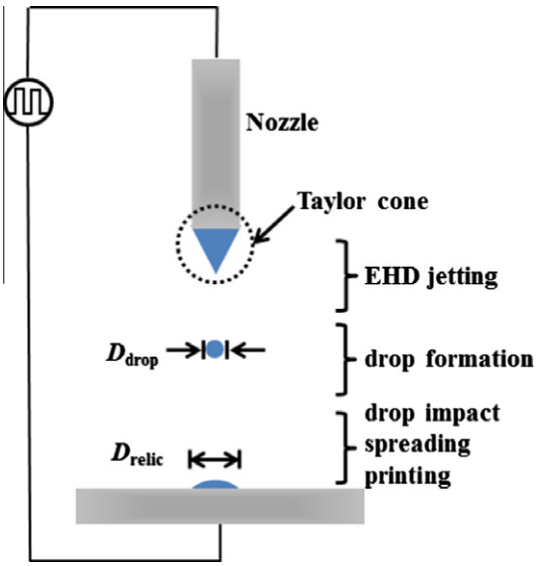

Fig. 1. Schematic of the EHD inkjet printing setup.

eventually droplet emission. The size of the droplet can be controlled by tuning the frequency of the applied voltage. The following parameters control the jetted droplet size and velocity: frequency (f), applied voltage (V), free space permittivity (ε_o), and fluid surface tension (σ) and viscosity (ν) [22–24]. Ejected charged droplets deposit onto a substrate through a process known as electrowetting [25].

Fig. 2 shows the inks used in the experiments. The Ag ink contains silver nano-particles well dispersed in an alcohol-based solvent, triethylene glycol monoethyl ether (TGME), whose properties are summarized in Table 1. Mean Ag colloid diameter is 40 nm and they are fairly monodisperse. The weight ratio of silver particles to TGME solvent is 32%. A diethylene glycol (DEG)-based ink with Al particles (mean size of 5–10 μm) is also shown in Fig. 2 (right). Although some studies show that ink conductivity can be dependent upon the concentration and size of suspended metal particles [26,27], DEG with Al particles did not show an increase in conductivity compared to pure DEG. Because the Al particles are two to three orders of magnitude larger than the Ag particles, they quickly settle (within 5–10 min). This poor dispersivity is the primary drawback of the Al ink; adding a dispersant

Fig. 2. Ag (left) and Al (right) ink suspensions.

Table 1
Properties of Ag and Al ink suspensions at 20 °C.

	Ag ink	Al ink (DEG base)	Al ink (ethanol base)
Density, ρ (kg/m^3)	1483	1118	789
Viscosity, μ (mPa s)	9	38.5	1.2
Surface tension, σ (mN/m)	32.5	44.8	22.1
Capillary speed, σ/μ (m/s)	3.61	1.16	18.4
$Re = \rho UD/\mu$	$52 < Re < 75$	$16 < Re < 24$	$260 < Re < 310$
$We = \rho U^2 D/\sigma$	$20 < We < 22$	$27 < We < 34$	$19 < We < 33$
$Oh = We^{0.5}/Re$	$0.06 < Oh < 0.09$	$0.24 < Oh < 0.35$	$0.01 < Oh < 0.02$
$Ca = We/Re$	$0.29 < Ca < 0.48$	$1.33 < Ca < 2.03$	$0.06 < Ca < 0.12$

might help, but this was not done in these experiments. While the high dispersion quality of nano-Ag is preferable, it is expensive. Fortunately, for standard printing resolutions (i.e., 10^{-1}–10^{0} mm), the relatively large size of the Al particles (a few microns) does not degrade the overall printing resolution.

Fig. 3 depicts the experimental setup of our EHD printing system. The Al ink, comprising Al particles in either DEG or ethanol, was supplied to a stainless-steel nozzle (EFD, 18 gauge, inner and outer diameters are 0.84 and 1.27 mm, respectively) by a syringe pump (KDS 100). A multi-function synthesizer (NF Corporation, WF 1973) generated a rectangular step-function signal, which was sent to the HV-amplifier (TREK 50/750) for thousand-fold amplification. The width of the rectangular signal (duty ratio) was held constant at 2 ms, which was 0.2% of the time when $f = 1$ Hz and 2% of the time when $f = 10$ Hz. Given the 2-ms duty ratio, frequencies in excess of 500 Hz were not possible here. Although higher frequencies could be imposed with a commensurately shorter duty ratio, it would preclude a consistent comparison of the controlling parameters on droplet properties. In this work, no baseline (or bias) low-voltage was applied, although this could facilitate preloading of the liquid meniscus for easier droplet ejection at each voltage peak. Li [28] showed the effect of the voltage pulse characteristics (such as amplitude, width, and bias-voltage level) on the shape of the meniscus while using a pure ethanol as a working fluid that contained no suspension particle. The studies on the voltage pulse characteristics (i.e., pulse duration and magnitude) for suspension inks are beyond the scope of the current study.

A high-speed camera (Vision Research, Inc., Phantom 7.3) assembled with zoom lens (1.56 μm/pixel) and Halogen lamp (250 W) captured magnified images of the jetting inks. Snapshots were taken at 200-μs intervals. The motorized stage or substrate (Future Science, FS-XY-0.1-100) can maneuver up to a maximum distance of 100 mm in 0.1-μm increments. The distance between the nozzle tip and the substrate was fixed at 5 mm. Excessive or insufficient voltage supply may destabilize the Taylor cone. The optimal voltage supply that yields a stable Taylor cone changes whenever the ink electro-fluid properties are changed (R1-3) (e.g., 7.5–10 kV in these experiments with more viscous fluids requiring higher voltage to eject ink droplets).

3. Results and discussion

Fig. 4 shows the effect of voltage frequency on an EHD jet of Ag ink for frequencies from 1 to 10 Hz. The snapshots taken at 1 Hz (Fig. 4a) shows that the ejected fluid was initially dumbbell-shaped (which has the potential to yield satellite droplets), but eventually it coalesced into a spherical droplet before impact. For low frequencies, the occasional satellite droplet was formed (R2-1) due to the nonlinear effect of the Rayleigh instability when capillary waves arise along the ejected fluid [29–32]. Upon impact, a droplet

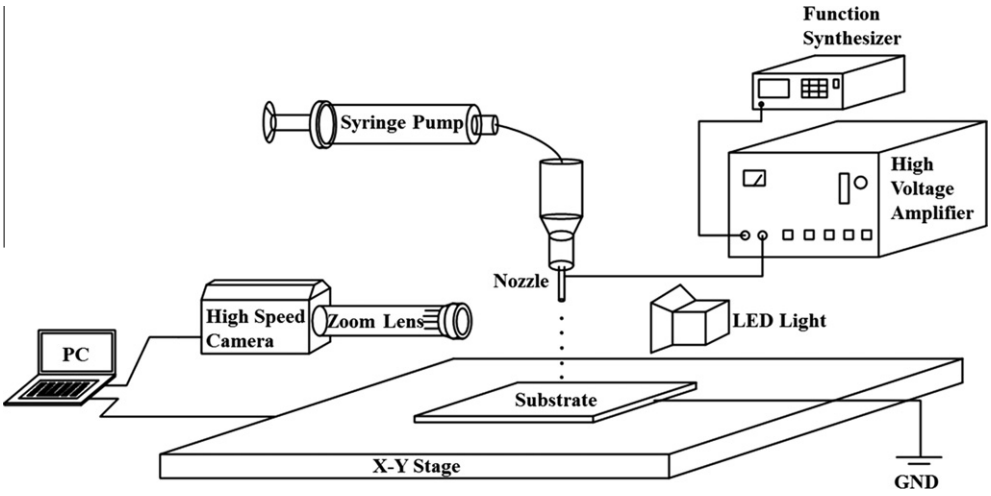

Fig. 3. Schematic of the EHD experimental setup.

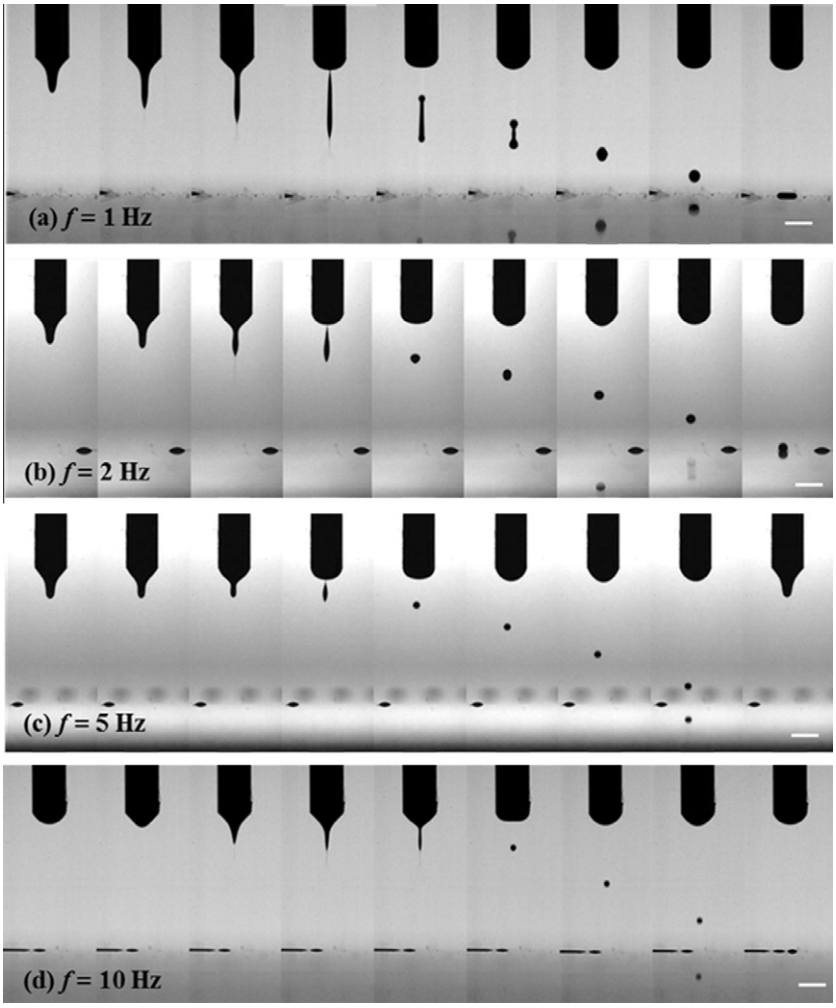

Fig. 4. EHD Ag ink droplet ejection at f = 1, 2, 5, and 10 Hz (Δt = 1 ms, scale bar = 1 mm).

spreads into a "relic" that is a few times larger than the incipient droplet. When the frequency was increased to 10 Hz (Fig. 4d), droplets became smaller. Furthermore, satellite droplets did not form because the EHD-induced wave was much shorter than the capillary wave.

Fig. 5 shows the deviation from droplet-on-demand for droplet generation rates and pulse frequencies less than 80 Hz. The droplet generation rate and the pulsing frequency matched (perfect droplet-on-demand) for frequencies up to about 40 Hz. However, deviation was observed for frequencies $f \geqslant 40$ Hz, which was

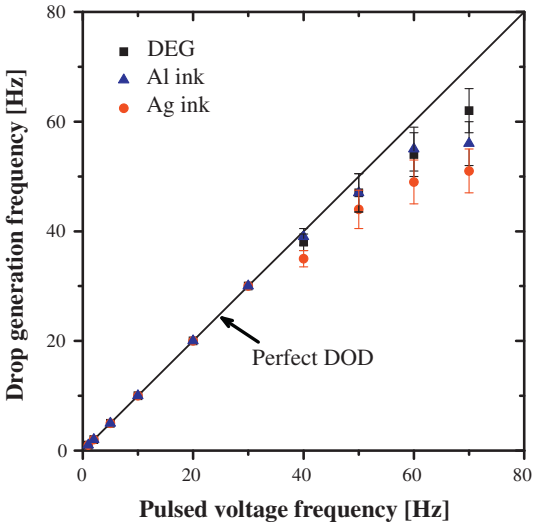

Fig. 5. Correlation between droplet generation and voltage frequency.

attributed to the fluid relaxation time. (R2-2) Note that the deviation is inherently present in all types of inkjets. It is well known that the charge relaxation time is inversely proportional to the fluid electrical conductivity, $\tau_e \sim 1/K$ [33–36]. Thus, in theory, the perfect conductor has zero relaxation time, which should in principle respond immediately to the supplied electrical charges. However, in reality, other factors, such as fluid viscosity and surface tension, hinder the immediate respond of the droplet that is electrically-driven. All of these coupled effects contribute to the deviation from the ideal line.

At higher frequencies, the natural frequency of the conical liquid meniscus cannot keep up with the imposed voltage fluctuations. Because no liquid is a perfect conductor and there is finite density and viscosity, high frequency voltages cannot be perfectly reflected in the droplet ejection rate. (R2-3) Paine [37] showed that there is an optimal voltage level for a stable operation of an electrospray while Lee et al. [38] showed the stable voltage range for an EHD inkjet mode. The inconsistency between the droplet generation rate and pulsing frequency is a common problem in inkjet technology. For example, Mishra et al. [39] printed the letter "I" with 2200 droplets over 70 s when the imposed frequency was 1 kHz (a droplet generation rate of merely 31 Hz).

Fig. 6 shows the effect of particle concentration, fluid viscosity, and voltage frequency on droplet characteristics. The Figs in the first column are from the experimental work of Furbank and Morris [40]. Particle-laden fluid more often resulted in satellite forma-

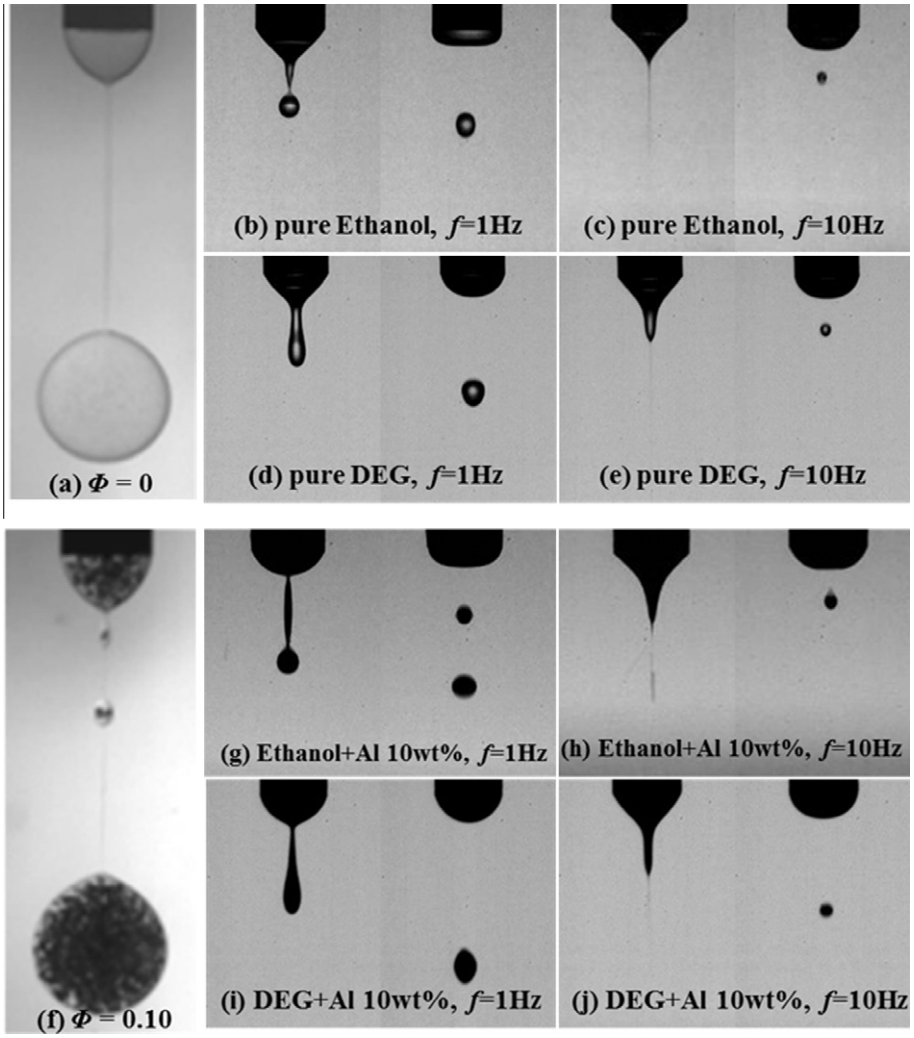

Fig. 6. The effect of various parameters (particle concentration, fluid viscosity, and voltage frequency) on droplet characteristics. The figures in the first column are from the experimental work of Furbank and Morris [40] (Reprinted under the permission of AIP.)

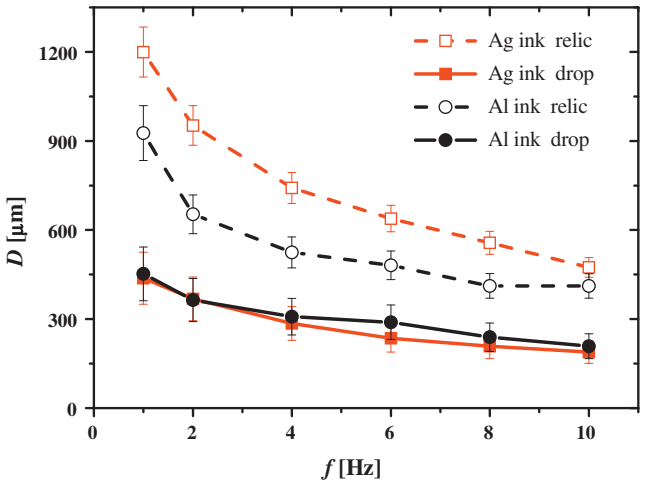

Fig. 7. Drop-size variation at various voltage frequencies for Ag and Al inks.

tion. Our EHD jet behaved similarly when the fluid was ethanol (low viscosity fluid). At a low viscosity (ethanol), the effects of surface tension (necking or thinning, so called singular behavior) are more pronounced. Fluid cohesion around particles yields satellites as the fluid necks and separates. Low-viscosity fluids (ethanol) are more prone to satellite droplet formation because of the increased relative importance of cohesion and surface tension. On the other hand, thinning (or necking) diminished for more viscous fluids (such as DEG). Increasing the solvent viscosity discouraged satellite formation and improved print quality. The stabilizing effect of viscosity in reducing satellite droplets was discussed by Hartman et al. [27] and Jayasinghe and Edirisinghe [22]. However, their studies focused on the cone-jet spray mode using a pure liquid without any suspended particles and thus their studies cannot be directly applied to our experiments. Without particles (pure liquid cases), satellites were unlikely to form regardless of the solvent viscosity because there are no particles for fluid to coalesce around. As viscosity increased (from ethanol to DEG), the role of surface tension was less pronounced, significantly reducing fluid necking. Further information on the capillary pinch-off of viscous fluids is available [41–46]. (R2-5) Kang et al. showed that the Al particle inclusion of 1–10 wt.% in DEG has no significant effect on fluid viscosity and electrical conductivity; hence the Al wt.% effect on the drop ejection characteristics such as impacting speed, drop size and drop separation distance from the nozzle tip was also negligible [47].

As expected, the droplet size was dependent upon the imposed EHD frequency; small droplets from high frequency [48,49]. Fig. 7 shows droplet size variation with EHD frequencies between 1 and 10 Hz. The inks are (1) DEG with 10% by weight Al and (2) a commercial Ag ink. Both the ejected droplet size and the size of the relic after printing were recorded. (R2-7) The Al ink data fall near the low end of the *x*-axis (compared to that of the Ag ink) because of DEG's larger surface tension and viscosity; see Table 1. The ejected droplet sizes of both Al and Ag inks are in the range of 150–450 μm. The Al ink relic size (300–900 μm) is 2–3 times larger than the initial droplet size and both relic and droplet sizes decrease when the frequency is increased. Voltage frequency seems to be the first-order driver for droplet size; other parameters (e.g., V, (R2-8)ε, σ, and ν) play relatively minor roles [48,49]. Ag ink relic sizes ranged from 600–1200 μm. However, the range of the relic size of the Al ink was smaller than that of Ag ink because DEG-based Al ink had higher surface tension and viscosity. Thus, inks with higher surface tension and viscosity are desirable if excessive spreading is to be avoided.

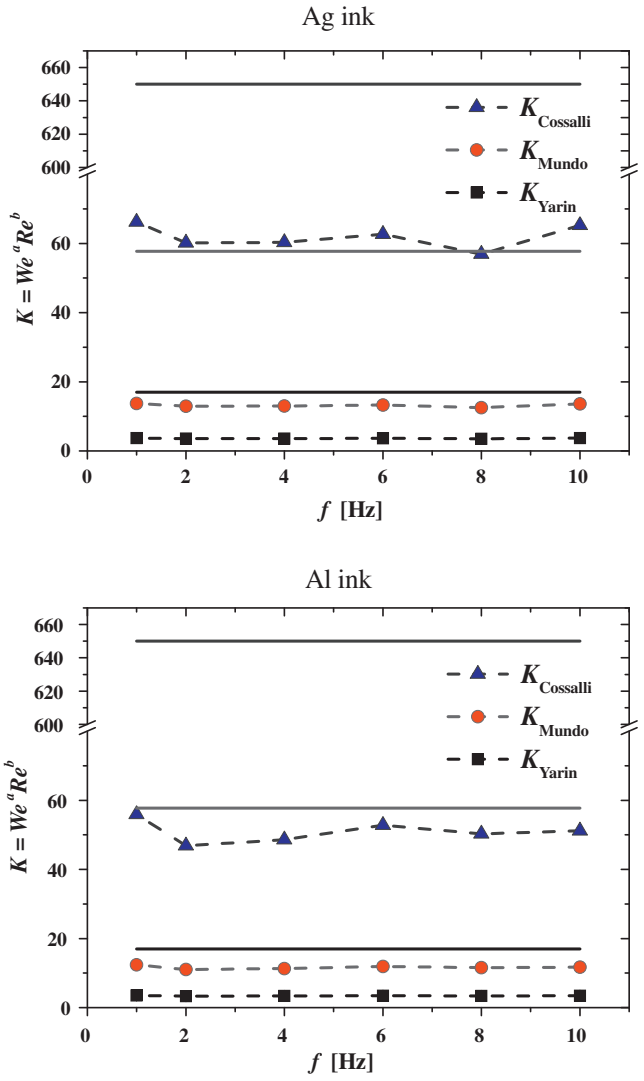

Fig. 8. Splashing potential for Ag (top) and Al (bottom) inks (10 wt.%). The critical impingement parameters offered by Yarin and Weiss [50], Mundo et al. [51], Cossali et al. [52] are $K_{crit(Yarin)} = We^{0.250}\ Re^{0.125} = 17$ (black line), $K_{crit(Mundo)} = We^{0.50}\ Re^{0.25} = 58$ (red line), and $K_{crit(Cossali)} = We^{0.8}\ Re^{0.4} = 650$ (blue line). None of our experimental data (both Ag and Al inks) showed any sign of splashing because the values are well below K_{crit}. (For interpretation of the references to color in this figure legend, the reader is referred to the web version of this article.)

For high-quality printing, splashing upon substrate impact should be minimized. In general, increasing EHD frequency reduces droplet size, but also increases the impact velocity. (R2-4) Smaller droplets are ejected with higher velocities due to the charge-to-mass ratio of the droplets that are under the influence of the imposed electrical field. Droplet-impact dynamics can be characterized by the Reynolds ($Re = \rho U/\nu$) and Weber number ($We = \rho U^2 D/\sigma$), where ρ, ν, σ, D, and U represent fluid's density, viscosity, surface tension, droplet diameter, and impact velocity, respectively. Yarin and Weiss [50], Mundo et al. [51], Cossali et al. [52] offered various splashing criteria including a critical impingement parameter ($K_{crit} = We^a\ Re^{a/2}$) above which splashing was likely; $K_{crit(Yarin)} = We^{0.250}\ Re^{0.125} = 17$, $K_{crit(Mundo)} = We^{0.50}\ Re^{0.25} = 58$, and $K_{crit(Cossali)} = We^{0.8}\ Re^{0.4} = 650$. None of our experiments showed any splashing. Fig. 8 shows that none of our cases exceeded K_{crit} supporting the observation that no splashing was observed during any of our printing efforts. Note that impact velocities (U) were estimated by measuring the distance traveled and

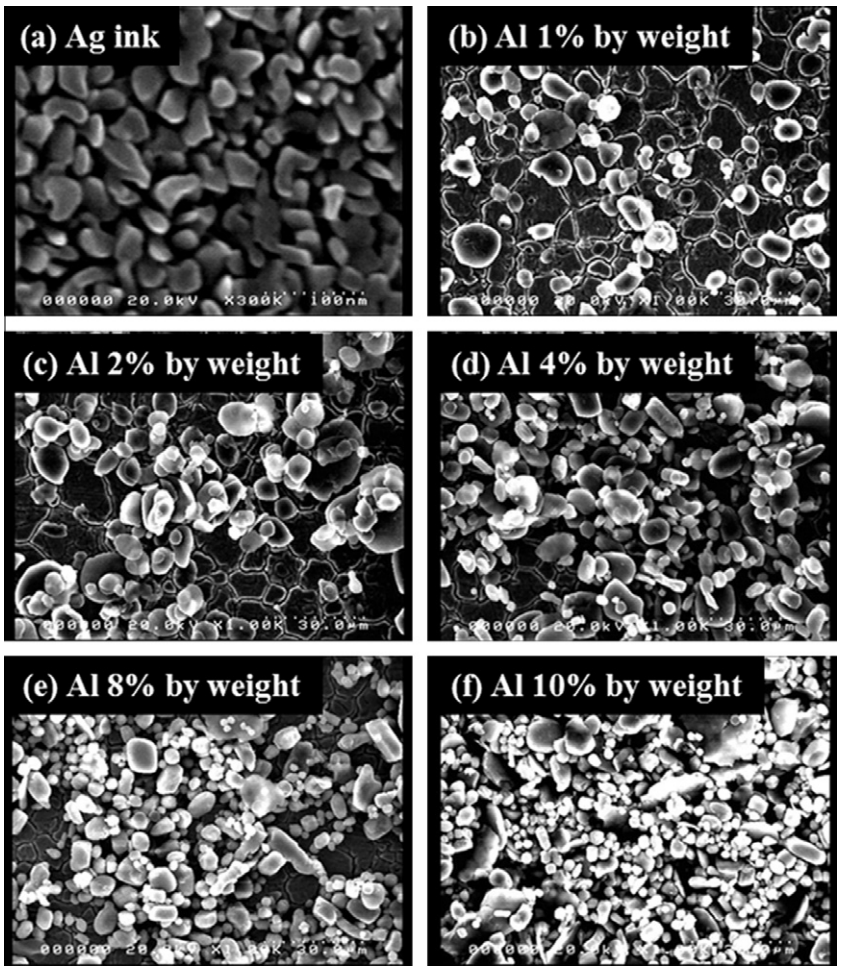

Fig. 9. SEM images of EHD-deposited inks containing Al and Ag particles.

the time interval between snapshots (using the Phantom 7.0, *Vision Research* high-speed camera) just before impact.

Relic particle concentrations are important; if the particle concentration is too low, then printed dots have decreased capacity as

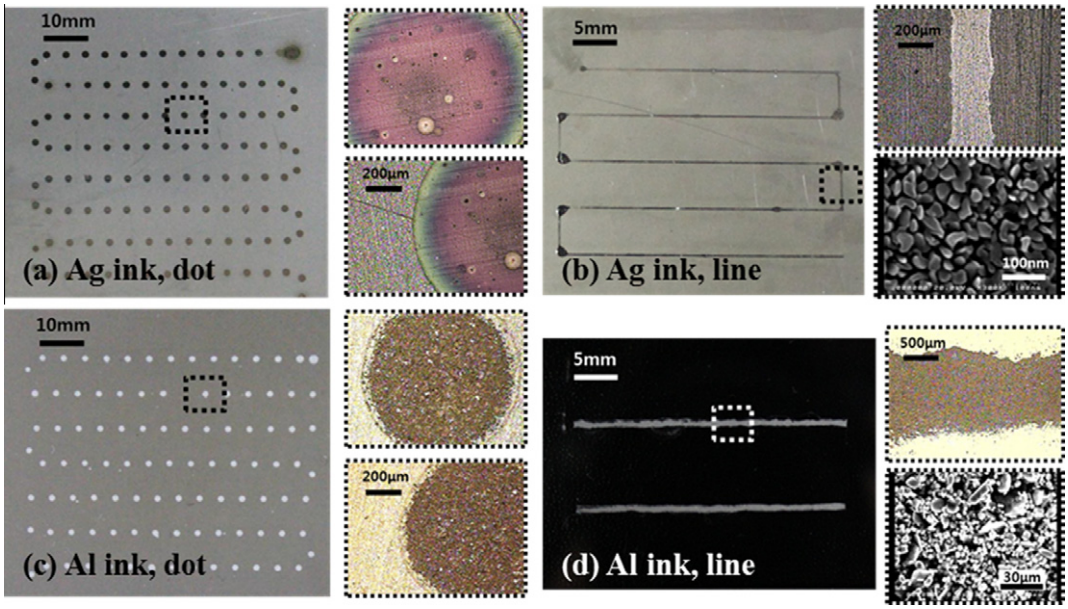

Fig. 10. Printed silver (top) and aluminum (bottom) powder on stainless and ITO substrates (DEG ink, Al 10% by weight, f = 1 Hz). The nozzle diameter is 0.84 and 0.25 mm for the dot and line printing, respectively. The line widths for the Ag and Al inks are 0.24 mm and 1.2 mm, respectively.

electrodes because a continuous flow of electrons cannot be supported. Fig. 9 shows scanning electron microscope (SEM) images of Ag and Al ink relics where particle concentration varied from 1% to 10% by weight. These images were taken after complete evaporation of the solvent. The commercial Ag ink (top-left) shows a compact arrangement of Ag nanoparticles (mean diameter is ~40 nm). When the Al particle concentration was low (1–4% by weight), relics were sparsely seeded and function as an electrode would be degraded. When Al particle loading reached 8% by weight, there was sufficient particle-number-density to form an effective electrode.

Fig. 10 compares dot and line printing performances of the commercial Ag ink and our Al ink (10% by weight). Magnified views of the printed relics after complete evaporation of the solvent for both Al and Ag inks are also shown in Fig. 10 (right Figs). Both an optical microscope and SEM were used to capture these snapshots.

For the dot printing results, the nozzle inner diameter was 840 μm, which ejected 150–450-μm droplets that formed relics in the 400–1200 μm range. The relic maintained the desired circular shape although the Al particles were not optimally dispersed (some aggregation was observed). Because Al particles are relatively large, the coffee ring effect (where nanoscale particles are driven toward the periphery of the relic due to internal circulation during evaporation [2,53,54]) was not observed. This is another advantage of using large particles (i.e., non-nanoscale) for EHD printing. (R2-6)This aluminum line was sintered at 500 °C in atmospheric and its resistivity was measured by taking the slope of the IV curve via the Ohm's Law ($I = V/R$); the resistivity was about ~90 Ω. Overall, our in-house, low-cost Al ink performed comparably to the expensive, commercial Ag-ink. This suggests that Al inks can replace the use of the more expensive commercial Ag ink for printing scales on the order of 100 μm. If finer printing scales (i.e., 10^0–10^1 μm) are required, then the Ag ink is a better choice.

To study a reduced printing scale, a smaller nozzle with a 240-μm diameter was used for line printing. Poorer line uniformity was achieved with the Al ink than with the Ag ink. Coalescence (or droplet-merging) took place between relics (i.e., printed dots), which tended to form a large puddle whose size as usually bigger than the size of an originally printed relic. The relatively large Al particles degraded line-printing quality. Coalescence induced internal flow circulation within droplets and hence flow-induced particle movement inside droplets was greatly hindered because of irregular size of Al particles. In addition, the largeness of Al particles also hindered the smooth transition of the coalescence process, resulting in relatively non-uniform line.

4. Conclusions

We demonstrated the feasibility of an in-house Al ink using EHD inkjet printing. Our low-cost inks with aluminum particles yielded reasonable performance on comparison with the expensive commercial ink comprised of silver nano-particles for an application of printing dots that are a few hundred microns in size. Characteristics of EHD inkjets were examined while varying the pulsing frequency, the ink viscosity and surface tension. Larger particles in the ink could potentially form satellite droplets that could degrade high-resolution printing quality. Satellite droplet formation can be diminished by increasing the ink viscosity. Droplet sizes were measured as functions of the frequency; the higher the frequency, the smaller the droplet size. Potential splashing upon impact was evaluated through several splashing criteria. There was no analytical or visual evidence of splashing, which is desirable for high quality printing. All of these EHD inkjet characteristics may be directly applicable for fabrication of microelectronics.

Acknowledgements

This study was supported by a grant from the cooperative R&D Program (B551179-08-03-00) funded by the Korea Research Council Industrial Science and Technology, Republic of Korea. This research was also supported by the Converging Research Center Program through the Ministry of Education, Science and Technology (2010K000969) and NRF-2012029433, NRF-2012-0001169, and NRF-2010-0010217.

References

[1] B.J.d. Gans, P.C. Duineveld, U.S. Schubert, Inkjet printing of polymers: state of the art and future developments, Adv. Mater. 16 (2004) 203–213.
[2] M. Singh, H.M. Haverinen, P. Dhagat, G.E. Jabbour, Inkjet printing—process and its applications, Adv. Mater. 22 (2010) 673–685.
[3] B.Y. Ahn, E.B. Duoss, M.J. Motala, X. Guo, S.I. Park, Y. Xiong, J.S. Yoon, R.G. Nuzzo, J.A. Rogers, J.A. Lewis, Omnidirectional printing of flexible, stretchable, and spanning silver microelectrodes, Science 323 (2009) 1590–1593.
[4] Z. Nie, E. Kumacheva, Patterning surfaces with functional polymers, Nat. Mater. 7 (2008) 277–290.
[5] B.J.d. Gans, U.S. Schubert, Inkjet printing of polymer micro-arrays and libraries: instrumentation, requirements, and perspectives, Macromol. Rapid Commun. 24 (2003) 659–666.
[6] S.R. Samarasinghe, I. Pastoriza-Santos, M.J. Edirisinghe, M.J. Reece, L.M. Liz-Marzán, Printing gold nanoparticles with an electrohydrodynamic direct-write device, Gold Bull. 39 (2006) 48–53.
[7] P. Tsai, S. Pacheco, C. Pirat, L. Lefferts, D. Lohse, Drop impact upon micro- and nanostructured superhydrophobic surfaces, Langmuir 25 (2009) 12293–12298.
[8] Z. Ahmad, E.S. Thian, J. Huang, M.J. Edirisinghe, S.M. Best, S.N. Jayasinghe, W. Bonfield, R.A. Brooks, N. Rushton, Deposition of nano-hydroxyapatite particles utilising direct and transitional electrohydrodynamic processes, J. Mater. Sci. 19 (2008) 3093–3104.
[9] F.C. Krebs, Polymer solar cell modules prepared using roll-to-roll methods: knife-over-edge coating, slot-die coating and screen printing, Sol. Energy Mater. Sol. Cells 93 (2009) 465–475.
[10] A.J. Lennon, R.Y. Utamaa, M.A.T. Lenioa, A.W.Y. Ho-Bailliea, N.B. Kueppera, S.R. Wenham, Forming openings to semiconductor layers of silicon solar cells by inkjet printing, Sol. Energy Mater. Sol. Cells 92 (2008) 1410–1415.
[11] M. Horteis, S.W. Glunz, Fine line printed silicon solar cells exceeding 20% efficiency, Prog. Photovoltaics 16 (2008) 555–560.
[12] P. Miao, P. Xiao, Formation of ceramic thin films using electrospray in cone-jet mode, ITIA 38 (2002) 50–56.
[13] A. Jaworek, A.T. Sobczyk, Electrospraying route to nanotechnology: an overview, J. Electrostat. 66 (2008) 197–219.
[14] K. Cheng, M.H. Yang, W.W. Chiu, C.Y. Huang, J. Chang, T.F. Ying, Y. Yang, Ink-jet printing, self-assembled polyelectrolytes, and electroless plating: low cost fabrication of circuits on a flexible substrate at room temperature, Macromol. Rapid Commun. 26 (2005) 247–264.
[15] N. Wu, L.F. Pease, W.B. Russel, Toward large-scale alignment of electrohydrodynamic patterning of thin polymer films, Adv. Funct. Mater. 16 (2006) 1992–1999.
[16] N. Wu, W.B. Russel, Micro- and nano-patterns created via electrohydrodynamic instabilities, Nano Today 4 (2009) 180–192.
[17] D.Z. Wang, S.N. Jayasinghe, M.J. Edirisinghe, High resolution print-patterning of a nano-suspension, J. Nanopart. Res. 7 (2005) 301–306.
[18] J.U. Park, M. Hardy, S.J. Kang, K. Barton, K. Adair, D.K. Mukhopadhyay, C.Y. Lee, M.S. Strano, A.G. Alleyne, J.G. Georgiadis, P.M. Ferreira, J.A. Rogers, High-resolution electrohydrodynamic jet printing, Nat. Mater. 6 (2007) 782–789.
[19] K. Sibel, A.S. Dudley, I.A. Aksay, Collodial cluster arrays by electrohydrodynamic printing, Langmuir 24 (2008) 12196–12201.
[20] D.Y. Lee, Y.S. Shin, S.E. Park, T.U. Yu, J.H. Hwang, Electrohydrodynamic printing of silver nanoparticles by using a focused nanocolloid jet, Appl. Phys. Lett. 90 (2007) 081905.
[21] G. Taylor, Disintegration of water drops in an electric field, Proc. Roy. Soc. A (1964) 383–397.
[22] S.N. Jayasinghe, M.J. Edirisinghe, Effect of viscosity on the size of relics produced by electrostatic atomization, J. Aerosol Sci. 33 (2002) 1379–1388.
[23] J.H. Yu, S.Y. Kim, J. Hwang, Effect of viscosity of silver nanoparticle suspension on conductive line patterned by electrohydrodynamic jet printing, Appl. Phys. A 89 (2007) 157–159.
[24] J.Y. Choi, Y.J. Kim, S. Lee, S.U. Son, H.S. Ko, V.D. Nguyen, D.Y. Byun, Drop-on-demand printing of conductive ink by electrostatic field induced inkjet head, Appl. Phys. Lett. 93 (2008) 193508–193510.
[25] F. Mugele, M. Duits, D. Ende, Electrowetting: a versatile tool for drop manipulation, generation, and characterization, Adv. Colloid Interface Sci. 161 (2010) 115–123.
[26] R. Jurascheka, F.W. Röllgen, Pulsation phenomena during electrospray ionization, Int. J. Mass Spectrom. 177 (1998) 1–15.

[27] R.P.A. Hartman, D.J. Brunner, D.M.A. Camelot, J.C.M. Marijnissen, B. Scarlett, Jet break-up in electrohydrodynamic atomization in the cone-jet mode, J. Aerosol Sci. 31 (2000) 65–95.
[28] J.L. Li, On the meniscus deformation when the pulsed voltage is applied, J. Electrostat. 64 (2006) 44–52.
[29] P. Lafrance, Nonlinear breakup of a liquid jet, Phys. Fluids 17 (1974) 1913.
[30] A.H. Nayfeh, Nonlinear stability of a liquid jet, Phys. Fluids 2 (1970) 841–847.
[31] M.C. Yuen, Non-linear capillary instability of a liquid jet, J. Fluid Mech. 33 (1968) 151–163.
[32] H. Park, S.S. Yoon, S.D. Heister, On the nonlinear stability of a swirling liquid jet, Int. J. Multiphase Flow 32 (2006) 1100–1109.
[33] P.K. Notz, O.A. Basaran, Dynamics of drop formation in an electric field, J. Colloid Interface Sci. 213 (1999) 218–237.
[34] R.T. Collins, M.T. Harris, O.A. Basaran, Breakup of electrified jets, J. Fluid Mech. 588 (2007) 75–129.
[35] R.T. Collins, J.J. Jones, M.T. Harris, O.A. Basaran, Electrohydrodynamic tip streaming and emission of charged drops from liquid cones, Nat. Phys. 4 (2008) 149–154.
[36] M.W. Lee, N.Y. Kim, S.S. Yoon, On pinchoff behavior of electrified droplets, J. Aerosol Sci., 2013, in press.
[37] M.D. Paine, Transient electrospray behaviour following high voltage switching, Microfluid Nanofluid. 6 (2009) 775–783.
[38] M.W. Lee, D.K. Kang, N.Y. Kim, H.Y. Kim, S.C. James, S.S. Yoon, A study of ejection modes for pulsed-DC electrohydrodynamic inkjet printing, J. Aerosol Sci. 46 (2012) 1–6.
[39] S. Mishra, K.L. Barton, A.G. Alleyne, P.M. Ferreira, J.A. Rogers, High-speed and drop-on-demand printing with a pulsed electrohydrodynamic jet, J. Micromech. Microeng. 20 (2010) 095026–095033.
[40] R.J. Furbank, J.F. Morris, An experimental study of particle effects on drop formation, Phys. Fluids 16 (2004) 1777–1790.
[41] X.D. Shi, M.P. Brenner, S.R. Nagel, A cascade of structure in a drop falling from a faucet, Science 265 (1994) 219–222.
[42] D.M. Henderson, W.G. Pritchard, L.B. Smolka, On the pinch-off of a pendant drop of viscous fluid, Phys. Fluids 9 (1997) 3188–3200.
[43] D.R. Webster, E.K. Longmire, Jet pinch-off and drop formation in immiscible liquid–liquid systems, Exp. Fluids 30 (2001) 47–56.
[44] A.U. Chen, P.K. Notz, O.A. Basaran, Computational and experimental analysis of pinch-off and scaling, Phys. Rev. Lett. 88 (2002) 174501.
[45] A. Rothert, R. Richter, I. Rehberg, Formation of a drop: viscosity dependence of three flow regimes, New J. Phys. 5 (2003) 59.
[46] J. Eggers, Drop formation – an overview, J. Appl. Math. Mech. 85 (2005) 400–410.
[47] D.K. Kang, M.W. Lee, H.Y. Kim, S.C. James, S.S. Yoon, Electrohydrodynamic pulsed-inkjet characteristics of various inks containing aluminum particles, J. Aerosol Sci. 42 (2011) 621–630.
[48] K. Tang, A. Gomez, Monodisperse electrosprays of low electric conductivity liquids in the cone-jet mode, J. Colloid Interface Sci. 184 (1995) 500–511.
[49] S.N. Jayasinghe, M.J. Edirisinghe, Electrostatic atomization of a ceramic suspension at pico-flow rates, Appl. Phys. A 80 (2005) 399–404.
[50] A.L. Yarin, D.A. Weiss, Impact of drops on solid surfaces: self-similar capillary waves, and splashing as a new type of kinematic discontinuity, J. Fluid Mech. 283 (1995) 141–173.
[51] C. Mundo, M. Sommerfeld, C. Tropea, Droplet-wall collisions: experimental studies of the deformation and breakup process, Int. J. Multiphase Flow 21 (1995) 151–173.
[52] G.E. Cossali, A. Coghe, M. Marengo, The impact of a single drop on a wetted solid surface, Exp. Fluids 22 (1997) 463–472.
[53] J.H. Park, J.H. Moon, Control of colloidal particle deposit patterns within picoliter droplets ejected by ink-jet printing, Langmuir 22 (2006) 3506–3513.
[54] C.H. Chon, S. Paik, J.B. Tipton Jr., K.D. Kim, Effect of nanoparticle sizes and number densities on the evaporation and dryout characteristics for strongly pinned nanofluid droplets, Langmuir 23 (2007) 2953–2960.